Prospects for generating electricity by large onshore and offshore wind farms

2017 Environ. Res. Lett. 12 034022

(http://iopscience.iop.org/1748-9326/12/3/034022)

Environmental Research Letters

LETTER

Prospects for generating electricity by large onshore and offshore wind farms

Patrick J H Volker, Andrea N Hahmann, Jake Badger and Hans E Jørgensen

Department of Wind Energy, Technical University of Denmark, Frederiksborgvej 399, 4000 Roskilde, Denmark

E-mail: pvol@dtu.dk

Keywords: Wind energy, Renewable energy, Mesoscale modelling, Resource estimation

OPEN ACCESS

RECEIVED
25 November 2016

REVISED
19 January 2017

ACCEPTED FOR PUBLICATION
1 February 2017

PUBLISHED
16 March 2017

Abstract

The decarbonisation of energy sources requires additional investments in renewable technologies, including the installation of onshore and offshore wind farms. For wind energy to remain competitive, wind farms must continue to provide low-cost power even when covering larger areas. Inside very large wind farms, winds can decrease considerably from their free-stream values to a point where an equilibrium wind speed is reached. The magnitude of this equilibrium wind speed is primarily dependent on the balance between turbine drag force and the downward momentum influx from above the wind farm. We have simulated for neutral atmospheric conditions, the wind speed field inside different wind farms that range from small (25 km^2) to very large (10^5 km^2) in three regions with distinct wind speed and roughness conditions. Our results show that the power density of very large wind farms depends on the local free-stream wind speed, the surface characteristics, and the turbine density. In onshore regions with moderate winds the power density of very large wind farms reaches 1 W m^{-2}, whereas in offshore regions with very strong winds it exceeds 3 W m^{-2}. Despite a relatively low power density, onshore regions with moderate winds offer potential locations for very large wind farms. In offshore regions, clusters of smaller wind farms are generally preferable; under very strong winds also very large offshore wind farms become efficient.

Introduction

To reach the recently agreed long-term goal of keeping the increase in global average temperature to well below 2 °C above pre-industrial levels, countries need to dramatically increase their use of renewable energy, such as the electricity generated from wind farms. To realise such increases, wind farms must continue to provide efficient power generation even when covering large areas.

A wind turbine removes kinetic energy from the atmospheric flow, which reduces the wind speed in its wake. A single turbine wake can extend for hundreds of rotor diameters downstream (Rados *et al* 2001). In a wind farm the velocity is further reduced by successive turbine wakes until the downward influx of momentum from above the wind farm balances the turbine's drag force. Despite the reduced power production of the inner turbines in a wind farm compared to those experiencing undisturbed free-stream wind speeds, current offshore wind farms (covering areas up to 10^2 km^2) have high capacity factors (ratio between the actual capacity over a period of time and the nameplate capacity over the same period) that are usually between 40% and 50% (LORC 2016).

With increasing wind farm sizes, however, the ratio between power production with and without wake effects is bound to decrease. It is thus important to determine whether future wind farms that cover large areas will remain sufficiently productive.

Several studies have analysed the global limits of wind energy extraction (Archer and Jacobson 2005, Jacobson and Archer 2012, Lu *et al* 2009, Marvel *et al* 2013), but did not investigate the degree to which the power production can be locally reduced in a very large wind farm. Other studies (Adams and Keith 2013, Miller *et al* 2015) focused on the regional limits of wind energy extraction. The results of their regional atmospheric model simulations suggested that 1 W m^{-2} is the maximum power per wind farm area (hereafter simply 'farm power density') that can

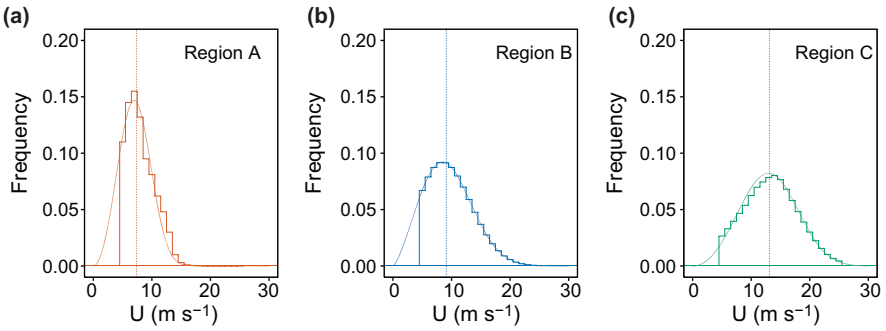

Figure 1. Hub-height wind speed frequency distribution for the onshore region with: (*a*) moderate winds (median wind speed of 7.4 m s^{-1}) and for the offshore regions with (*b*) strong winds (median wind speed of 9.1 m s^{-1}) and (*c*) very strong winds (median wind speed of 13.1 m s^{-1}). The smooth line shows the Weibull distribution fit to that distribution and the vertical dashed line the median wind speed.

be extracted from the atmosphere by very large wind farms (10^4 to 10^5 km^2). The existence of such limit would imply that the farm power density of very large wind farms compared with current existing wind farms will be reduced by up to 50% onshore (MacKay 2013) and up to 75% offshore (Petersen *et al* 2013).

The objective of this work is to study the potential of wind energy extraction in three regions with distinct wind and surface conditions (land and water). We use regional atmospheric model simulations to analyse the wind speed field and to assess the power density in the limit of very large wind farms for each region. Then, we perform experiments for various wind farm layouts to identify for each region the most appropriate wind farm type in terms of efficiency (ratio between power production with and without wake effects) and associate this with the annual energy production (AEP) that can be achieved.

Methods

We used the Weather Research and Forecast (WRF) model (Skamarock *et al* 2008) V3.4 to simulate the velocity field inside wind farms in three regions with different wind conditions, referred to as Region A (onshore), B (offshore), and C (offshore) in figure 1. The simulations are designed to understand how the time-averaged velocity reduction in very large wind farms depends on the free-stream wind, the surface roughness length, and the turbine spacing. From the velocity reduction in very large wind farms, we determine the degree to which the power density—in the limit of very large wind farms—depends on regional conditions. Furthermore, the results are used to determine which wind farm type in terms of wind farm size and turbine density would be most efficient in a given region.

Real versus idealised simulations

Simulations using the WRF model can be run in 'real' or 'idealised' mode. In the real mode e.g. reanalysis data are used to define the initial state and the time-varying boundary values of the model domain. The time-averaged wind speed field is then computed explicitly from a long period of simulations. In the idealised mode initial conditions are uniform across the domain. The lateral boundary conditions can be periodic, symmetric, or open and are without external forcing. The time-averaged wind speed is then obtained by a—region dependent—weighted average of steady-state simulations with different wind speeds.

We used the idealised mode to simulate the time-averaged wind speed field inside wind farms for three regions with distinct wind speed conditions above a homogeneous surface roughness. This choice has the advantage that the results are valid for any region with a comparable wind speed distribution and a similar, homogeneous, surface roughness. For regions with large variability in roughness or orography, the idealised mode is not recommended and a long-term real mode simulation should be conducted. An additional advantage of the idealised simulations is that they are computationally inexpensive and the mechanisms that control the time-averaged flow field within wind farms can be systematically examined. This is not possible in the real mode simulations because the wind speed and direction are constantly varying. Volker *et al* (2015) successfully uses the idealised mode to simulate the time-averaged wind speed of the Danish offshore wind farm Horns Rev I and Badger *et al* (2014) applies a similar method for wind resource assessment.

Wind speed distributions

The idealised simulations were run until a steady-state wind speed was reached (for details see Volker *et al* 2015). To obtain the region dependent time-averaged flow, we performed simulations with converged wind speeds between the cut-in (wind speed at which turbines begin to produce electricity) and cut-out (wind speed at which turbines shut down to avoid damage) wind speed in 1 m s^{-1} intervals. The time-averaged wind speed for each region was calculated by weighting the individual simulations with a prescribed wind speed distribution (figure 1).

The wind speed distribution of Region A, with a median wind speed of 7.4 m s^{-1}, was obtained from a one year WRF simulation in the USA State of Iowa. These wind conditions, which are characteristic for onshore regions with a homogeneous roughness, as the U.S. Great Plains or the Pampas of Argentina, are referred to as 'moderate'. The distribution of the offshore Region B, with a median wind speed of 9.1 m s^{-1}, was obtained at Horns Rev (Denmark) from a multiple year (2006–2011) WRF simulation over the North Sea (Hahmann *et al* 2015). We refer to regions with similar wind conditions (e.g. the USA Pacific Northwest) as areas with 'strong' wind speeds. The wind speed distribution of Region C, with a median wind speed of 13.1 m s^{-1}, was obtained from long-term (1979–2013) Modern-Era Retrospective analysis for Research and Applications (MERRA) data (Rienecker and Coauthors 2011). It represents offshore areas such as the Strait of Magellan, the Gulf of Suez in Egypt, Lake Turkana in Kenya or the Somalian Indian Ocean coast. Here, we refer to Region C as an area with 'very strong' winds.

Modelling of wind farms

Wind farm parametrisations used in mesoscale models add in each turbine-containing grid-cell a volume-averaged drag force to the model's flow equations. Due to the coarse horizontal resolution of these models, it is not possible to simulate local, instantaneous, flow reductions between turbines that depend on the wind direction and turbine positions (Jiménez *et al* 2015, Wu and Porté-Agel 2011). However, it has been shown that using these parametrisations the modelled wind speed inside an offshore wind farm with regularly spaced turbines verifies very well with time and wind direction averaged wind speed measurements (Volker *et al* 2015). Here, we used the Explicit Wake Parametrisation (EWP) scheme, introduced in Volker *et al* (2015). This approach requires a free initial length scale parameter σ_o. We chose an initial length scale of $\sigma_o = 1.7\ R_0$, since this value was found to be optimal under neutral atmospheric stability conditions in Volker *et al* (2015). We have also repeated all simulations using the WRF wind farm (WRF-WF) scheme (Fitch *et al* 2012) to explore the sensitivity of the wind farm flow to the wind farm parametrisation.

All hypothetical wind farms are equipped with Vestas V80 2 MW wind turbines with a 70 m hub-height. These turbines have a 80 m rotor diameter (D_0) and produce electricity when the wind speed is between 4 and 25 m s^{-1}. Their thrust and power curve information was obtained from the WAsP programme (Mortensen *et al* 2007). We defined four square-shaped hypothetical wind farms with sizes: small (5 km × 5 km), medium (18.5 km × 18.5 km), large (170 km × 170 km), and very large (338 km × 338 km). The size of our very large wind farms ($1.1{\cdot}10^5$ km^2) was chosen to be comparable to the large wind farms ($2.7{\cdot}10^5$ km^2) in Adams and Keith (2013).

Table 1. Total number of turbines of the various wind farms as a function of wind farm size and turbine spacing used in the model simulations. D_0 denotes the rotor diameter.

	Small	Medium	Large	Very large
Wide (10.5 D_0)	6 × 6	22 × 22	202 × 202	402 × 402
Intermediate (7 D_0)	9 × 9	33 × 33	303 × 303	603 × 603
Narrow (5.25 D_0)	12 × 12	44 × 44	404 × 404	804 × 804

For each wind farm size, we used three turbine spacings: wide (840 m or 10.5 D_0), intermediate (560 m or 7 D_0), and narrow (420 m or 5.25 D_0). The total number of turbines in each wind farm is listed in table 1.

The following examples provide some reference regarding the scales of the wind farms. The offshore wind farm Horns Rev I, which has been operational since 2002 and contains 80 2 MW turbines on 20 km^2 (LORC 2016), corresponds in our set-up to a small size wind farm. The largest offshore wind farm in 2016, the London array, that consists of 175 3.6 MW turbines on 100 km^2 (LORC 2016), is smaller than what we consider medium size in our set-up. To put into perspective the magnitude of the wind farms in our set-up, the total number of turbines in the very large wind farm with intermediate turbine spacing is close to the 314000 turbines currently installed worldwide (GWEC 2016).

We determined the power production from the simulations with a wind farm as follows. First, with the V80 power curve, $P(U)$, we prepared a look-up table of the power-coefficient, $C_p(U) = P(U)/(0.5\,\rho\,\pi\,R_0^2\,U^3)$, where ρ is the air density provided by the turbine manufacturer, R_0 is the length of the blades, and $U = U_{hh,\infty}$ is the free-stream wind speed at hub-height. Then, during the simulation, the actual power density (APD) of the wind farm, P_a, was obtained with,

$$P_a = \frac{1}{2}\frac{\rho_a \pi R_0^2}{A} \sum_{i=1}^{N_w} f_i \sum_{j=1}^{N_T} C_p(U_j)\, U_j^3, \quad (1)$$

where ρ_a =1.224 kg m^{-3} is the air density of the dry standard atmosphere ($T = 15^\circ$ and $P = 1013$ hPa), A is the wind farm area, i is the index of the wind speed bin, j is the turbine index, N_w is the number of wind speed bins, N_T is the number of turbines in the wind farm, f_i is the frequency of wind speed bin i, U_j is the wind speed at the hub-height (70 m) of turbine j. The reference power density (RPD) of a wind farm was obtained from equation (1) by using the undisturbed wind speed.

WRF model setup

The WRF model simulations were configured using 300 × 300 cells in the west-east and north-south direction with horizontal grid-spacing of 1.68 km. Forty levels were used in the vertical, with the first mass level at 10 m above the surface a total of 19 levels

Figure 2. Gemini wind farm located to the North of the Netherlands; this wind farm contains 150 Siemens 4MW turbines. Courtesy: Van Oord.

Table 2. WRF model configuration used in the simulations.

Domain size (x, y, z) (km):	504, 504, 15
Boundary condition:	OPEN (Skamarock *et al* 2008)
PBL scheme:	MYNN 2.5 (Nakanishi and Niino 2009)
Surface layer scheme:	MYNN Monin-Obukhov similarity theory
TKE advection:	Yes
Pert Coriolis:	Yes
Coriolis frequency (s^{-1})	$1.2 \cdot 10^{-4}$
Wind farm schemes	WRF-WF and EWP with $\sigma_0 = 1.7\ R_0$

were within the lowest 600 m. A surface roughness length of 0.1 m, which is typical for cropland, was used in the onshore simulations; in the offshore simulations we use the wind dependent Charnock relation (Charnock 1955). The wind speed converged from an initial constant geostrophic wind in height to a neutral logarithmic wind profile with and Ekman spiral in a 650 m deep boundary layer. Therefore, one should be careful when comparing the results to regions where the wind profile frequently deviates from that in neutral atmospheric conditions (e.g. USA Mid-West), since the power production depends on the wind shear across the rotor-disk (Vanderwende and Lundquist 2012, Wagner *et al* 2011).

The simulations were conducted for one wind direction. A study of the sensitivity to the wind direction showed a low sensitivity to the total power production for square wind farms, because single turbine wakes are not directly simulated in mesoscale models. We summarised the model configuration in table 2 and further details can be found in Volker *et al* (2015).

Results

Physical mechanisms that regulate power extraction

In large wind farms, turbines are mostly located within the wind shadow of upstream turbines (figure 2). Downstream from the first row of a wind farm, wind speeds can be considerably reduced because of successive turbine wakes that limit the amount of energy extracted by individual turbines. Inside wind farms, flow decelerations are caused by the turbine's drag, whereas accelerations in the wake of a turbine are controlled by the turbulent downward transport of

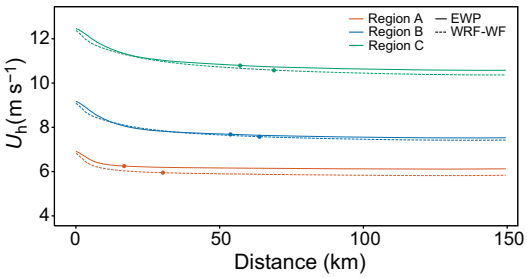

Figure 3. Simulated wind speed at hub-height for the EWP and WRF-WFwind farm parametrisation in the first 150 km of a very large wind farm ($1.1 \cdot 10^5$ km^2) with a wide turbine spacing (10.5 D_0) for the three wind climates in figure 1. The dots indicate the distance were the wind speed is 2% above the maximum velocity deficit.

momentum from the increased velocity shear in the wake (Adams and Keith 2013, Meyers and Meneveau 2012, Miller *et al* 2015, Porté-Agel *et al* 2014).

We model the wind farm flow with two wind farm schemes for neutral atmospheric conditions and account for a wind speed dependent surface roughness in the offshore regions with the Charnock relation. At the entrance of the wind farm, the wind speed in the two schemes is slightly different (figure 3). This is caused by the different parametrisation of the drag force in the two schemes that affects the permeability of the wind farm and, consequently, the wind speed reduction in front of the wind farm. Inside the wind farm, at a certain distance from the edge, where the turbine drag and the turbulent downward transport of momentum balance, an equilibrium wind speed is reached. In the onshore Region A, with high background turbulence levels caused by the rough land surface, the equilibrium wind speed is reached after a relatively short distance (i.e. 17 km in the EWP scheme and 30 km in the WRF-WF scheme). On the other hand, in the offshore Regions B and C the equilibrium wind speed is on average reached further downstream (i.e. 54 and 57 km in the Regions B and C for the EWP scheme) as a result of less background turbulence over the smooth water surface.

If the farm power density of very large wind farms were to be bounded to a universal value, as it has been

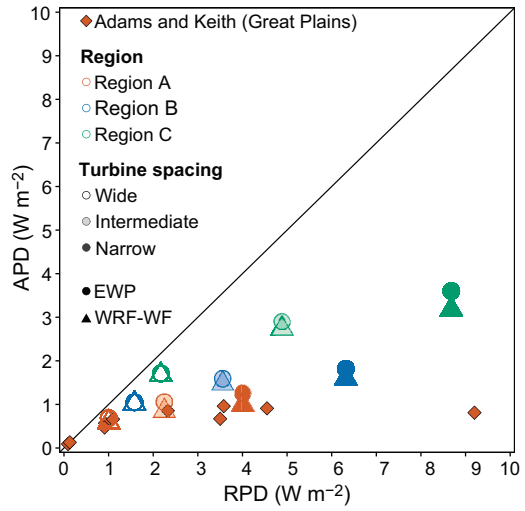

Figure 4. Actual power density (APD) versus the reference power density (RPD) for very large wind farms ($1.1 \cdot 10^5$ km^2) subject to three wind climates (figure 1). The transparency of the dots represents the turbine spacing. The results from Adams and Keith (2013) are in diamonds.

previously suggested (Adams and Keith 2013, Miller *et al* 2015), the wind speed would converge in all regions to the same asymptotic value. However, the simulations show that wind speed slows down to a region-dependent asymptotic wind speed because of various reasons. First, for conventional turbines as the V80 turbine the drag only increases in the range from the cut-in wind speed to approximately 12 m s^{-1}. At higher wind speeds, where the power production has nearly reached the rated power level, the turbine pitches its blades to reduce its drag. This results in smaller wind speed reductions in regions where rated power becomes more frequent. Second, the intensity of the turbulent momentum influx from velocity shear in the vertical direction depends on the surface roughness and the free-stream velocity. In regions with the same surface roughness, larger free-stream wind speed results in larger velocity shear. In regions with the same free-stream wind speed at a given height, larger surface roughness also results in larger velocity shear. Therefore, the wind speed reduction inside a wind farm and the magnitude of the equilibrium wind speed has a dependency on the region.

The degree to which the turbine drag reduces the wind farm power density (average power production per unit area) in a given region can be measured by comparing the actual power density (APD) with the reference power density (RPD), which is obtained when all turbines experience free-stream wind conditions. In each region, we analysed the behaviour of the APD for very large wind farms with the various turbine spacings (table 1).

Due to the absence of wakes, the RPD increases with stronger winds and a narrower turbine spacing, whereas the increase of APD depends on the degree to which the turbulent influx of momentum compensates the increased drag per unit of area (figure 4). In the onshore Region A with moderate winds the APD of a very large wind farm is limited to approximately 1 W m^{-2}. Thus, because of the relatively low free-stream wind speed, the power production per unit area of very large wind farms in onshore regions with moderate winds reaches this upper limit when the turbine spacing is less than intermediate. A further reduction of the turbine spacing does not increase the ADP. This result is in line with the farm power density of very large hypothetical wind farms in the USA Great Plains from Adams and Keith (2013), which used a similar wind farm parametrisation approach to the WRF-WF scheme. The farm power density simulated with the EWP scheme is generally slightly higher than with the WRF-WF scheme, but the tendencies are for both approaches the same. Figure 4 shows that in offshore Regions B and C not only the RPD of very large wind farms increases compared to that in the onshore Region A, but that also the APD becomes larger. In the offshore Region B the APD of the very large hypothetical wind farm reaches almost 2 W m^{-2} and it exceeds 3 W m^{-2} in the offshore Region C with very strong winds and narrow turbine spacing. The results indicate that the APD of very large wind farms is not limited to an universal value, but rather is strongly dependent on the regional free-stream wind conditions and on the turbine spacing.

Implications for wind farm development

So far we laid the grounds for determining the extent to which the atmosphere can supply energy to sustain the air flow within the wind farm. From the perspective of developers and energy policy makers, however, assessing the performance of the wind farm is an important consideration. We use efficiency, i.e. the ratio between power production with and without wake effects (Barthelmie and Jensen 2010), and the AEP to evaluate the performance of all wind farm configurations in the three regions. To our analysis, we include all wind farm sizes and turbine spacings listed in table 1. Here, we consider a wind farm to be efficient at a value close to or above 70%. This value corresponds approximately to the power losses in Horns Rev I for westerly winds of 8.0 ± 0.5 m s^{-1} (Barthelmie *et al* 2010). We present the results for the EWP scheme only; those for the WRF-WF scheme display the same tendencies.

Figure 5 and table 3 show the wind farm efficiency and AEP as a function of the wind farm area for all turbine spacings. In onshore regions with moderate winds (figure 5(*a*)), the efficiency of small and medium wind farms drops significantly with a decreasing turbine spacing. Thus, smaller wind farms with a narrow turbine spacing represent a relatively inefficient option, since already in small wind farms the turbulent influx of momentum is too weak to compensate the turbine's drag force when turbines are narrowly spaced. On the other hand, the efficiency of very large wind farms with a wide turbine spacing is

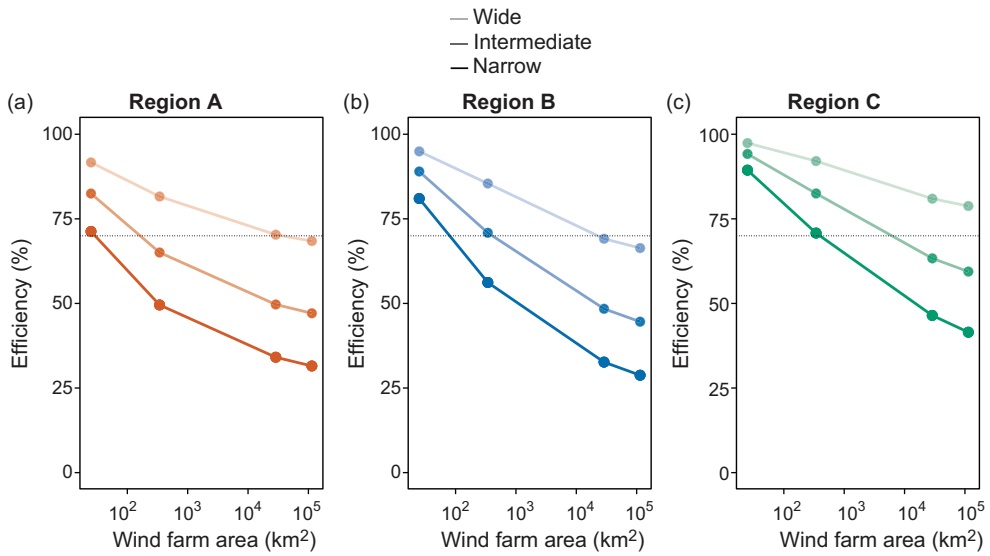

Figure 5. Wind farm efficiency for the EWP parametrisation as a function of the wind farm area in the: (*a*) onshore Region A, (*b*) the offshore Region B, and (*c*) the offshore Region C for the wide (10.5 D_0), intermediate (7 D_0), and narrow (5.25 D_0) turbine spacings (transparency). The efficiency of 70% is indicated with a dotted line.

Table 3. AEP (TWh) for the hypothetical wind farm sizes and turbine spacings in the three regions for the EWP parametrisation.

Turbine spacing	Small	Medium	Large	Very Large
		Region A		
Wide	$2.0 \cdot 10^{-1}$	2.5	$1.8 \cdot 10^2$	$6.9 \cdot 10^2$
Intermediate	$4.1 \cdot 10^{-1}$	4.4	$2.8 \cdot 10^2$	$1.1 \cdot 10^3$
Narrow	$6.4 \cdot 10^{-1}$	5.9	$3.5 \cdot 10^2$	$1.3 \cdot 10^3$
		Region B		
Wide	$3.3 \cdot 10^{-1}$	4.0	$2.8 \cdot 10^2$	$1.0 \cdot 10^3$
Intermediate	$7.0 \cdot 10^{-1}$	7.5	$4.3 \cdot 10^2$	$1.6 \cdot 10^3$
Narrow	1.1	$1.1 \cdot 10^1$	$5.2 \cdot 10^2$	$1.8 \cdot 10^3$
		Region C		
Wide	$4.7 \cdot 10^{-1}$	6.0	$4.4 \cdot 10^2$	$1.7 \cdot 10^3$
Intermediate	1.0	$1.2 \cdot 10^1$	$7.8 \cdot 10^2$	$2.9 \cdot 10^3$
Narrow	1.7	$1.8 \cdot 10^1$	$1.0 \cdot 10^3$	$3.6 \cdot 10^3$

comparable to that of small wind farms with a narrow turbine spacing. Despite the relatively low power density in onshore regions with moderate winds, a very large onshore wind farm with an AEP of 690 TWh would be powerful enough to supply nearly 17% of the 4087 TWh USA electrical consumption in 2015 (EIA 2015).

In offshore regions with strong free-stream winds (figure 5(*b*)), the winds can penetrate further into wind farms than in the onshore regions with moderate winds (figure 3), even when their turbine spacing is narrow. Hence, in small and medium wind farms all turbines benefit from the good wind conditions and are 5% to 10% more efficient than the same wind farms in onshore regions with moderate winds. Although large and very large wind farms in offshore regions with strong winds are exposed to stronger free-stream winds relative to those onshore, their efficiency decreases to lower levels compared to the same wind farms over land. This seemingly counter intuitive behaviour can be explained by the lower turbulent shear production levels over smoother water surfaces than over land (van der Laan *et al* 2015). In small and medium offshore wind farms, where the wind speed has still not reached the equilibrium wind speed, all turbines benefit from the good free-stream wind conditions. Whereas, large and very large offshore wind farms in Region B become less efficient than over land, due to the smaller momentum supply from aloft over smooth water surfaces. An offshore region with strong winds that is currently considered for extensive wind farm development is the Dogger Bank area ($1.5 \cdot 10^4$ km^2) in the North Sea. This shoal could support a cluster of nine medium-sized wind farms that are each 35 km apart. The AEP of this hypothetical wind farm cluster alone, where all individual wind farms with an intermediate turbine spacing benefit from free-stream wind conditions, would be approximately 68 TWh. This would cover more than 20% of the 331 TWh electricity consumption in the UK in 2014 (IEA 2014).

In offshore regions with very strong winds, the wind farm efficiency is always noticeably higher than that in the other considered regions (figure 5(*c*)). The wake losses of small wind farms are so small that the efficiency remains above 90% for each evaluated turbine spacing. One small wind farm with an intermediate 7 D_0 turbine spacing has the potential to produce 1 TWh, which is around 1.4 times the power production of the nearly identical Danish offshore wind farm Horns Rev I (Petersen *et al* 2013). Also for medium-sized wind farms with narrow turbine spacing the AEP is 47% higher than in the North Sea. Small- and medium-sized wind farms are especially advantageous in windy regions that are smaller geographically, such as the Gulf of Suez in Egypt or Lake Turkana in Kenya. In vast areas characterised by very strong winds, large or very large wind farms can be considered as well. The AEP of a hypothetical very large wind farm with a wide turbine

spacing could reach values of 1.7 PWh, which is sufficient to supply more than 7% of the 22 PWh global electricity consumption in 2014 (IEA 2014).

Summary and conclusions

With the rapid growth of wind power installations, it is increasingly important to investigate whether wind farms that cover large areas produce enough power to remain a competitive energy source.

We investigated whether the farm power density of very large wind farms is limited to certain values and related this to the wind farm efficiency and its AEP. We used the mesoscale model WRF in an idealised configuration to simulate the time-averaged velocity field in a neutral atmospheric boundary layer for various wind farm layouts in three regions. Because of the predefined wind speed distributions, we assume that there is no global feedback. Each of the three regions is characterised by a specific wind speed distribution and a flat surface with homogeneous roughness length. Therefore, the results are representative for any region with a similar wind speed distribution and relative homogeneous surface conditions, but are not applicable to regions with a complex orography and variable surface roughness length. For regions that are often exposed to non-neutral atmospheric stability (e.g. USA Great Plains) future investigation is needed to identify the influence of more pronounced wakes in stable conditions and less pronounced wakes in unstable conditions (Abkar *et al* 2016) on the AEP. Note that the power density in Region A and that from 'real' simulations in the USA Great Plains (Adams and Keith 2013) match well. For consistency, we used the Vestas V80 turbine for all of the square-shaped hypothetical wind farms, although modern offshore wind farms are often equipped with larger and more energy producing turbines (EWEA 2016) and have optimised layouts. In the future it will be interesting to investigate how the wind farm efficiency in different regions behaves for larger wind turbines and for new turbine technologies, such as low induction turbines (Schepers *et al* 2015).

Although our experiments are idealised (see methods), the simulated AEP with the EWP scheme matches closely the power production measurements of the Horns Rev I wind farm. The Horns Rev I wind farm (20 km^2) with 80 regularly spaced Vestas V80 turbines has a farm power density of 3.98 W m^{-2} (Petersen *et al* 2013), corresponding to 698 GWh. With the EWP wind farm parametrisation, the simulated wind farm in our set-up produces 700 GWh. Since currently no large or very large wind farms exist, we have assumed that the mechanisms regulating the flow inside large wind farms are similar to those in small wind farms and that consequently the power density is estimated correctly.

In the onshore region, with characteristics similar to that of the USA Great Plains, the farm power density is bounded to around 1 W m^{-2}. This is in line with previous studies (Adams and Keith 2013, Miller *et al* 2015). Despite the relatively low farm power density, the wind farm efficiency remains relatively high under the condition that the turbine spacing remains wide (10.5 D_0). Therefore, in these areas it would be more efficient to build one very large wind farm with a wide turbine spacing, instead of several separated smaller wind farms with a more narrow turbine spacing. The second region of our study was located offshore and had strong wind speeds, characteristic of the North Sea area. In 2015, the North Sea accounted for 63% of the global offshore wind capacity (12 GW) (EWEA 2016, GWEC 2016) and its total capacity is expected to increase further (4C Offshore 2016). For regions such as the North Sea, small or medium sized wind farms are more efficient than in onshore regions with moderate wind. Despite the strong winds, the efficiency of large and very large wind farms drops to lower values compared to onshore regions. Therefore, clusters of smaller wind farms are a better option in the North Sea, especially when their separation is large enough for each wind farm to benefit from undisturbed winds. Finally, we considered offshore regions with very strong winds, characteristic of the west opening of the Strait of Magellan. Although it is remote, this area offers a huge potential for future wind farms. Because of the very strong winds, small wind farms with efficiencies from 90%–98% would operate almost without wake losses. A small wind farm of 81 Vestas V80 turbines with an intermediate turbine spacing would produce annually around 1 TWh, which is more than 140% the power production of Horns Rev I. In these regions, even for very large wind farms the power density would exceed 3 W m^{-2}. The AEP of 1.7 PWh for one hypothetical very large wind farm with a wide turbine spacing corresponds to 7% of the global electricity consumption.

References

4C Offshore 2016 *4c offshore ltd* (http://www.4coffshore.com/offshorewind/)

Abkar M, Sharifi A and Porté-Agel F 2016 Wake flow in a wind farm during a diurnal cycle *J. Turbulence* **17** 420–41

Adams A S and Keith D W 2013 Are global wind power resource estimates overstated? *Environ. Res. Lett.* **8** 015021

Archer C L and Jacobson M Z 2005 Evaluation of global wind power *J. Geophys. Res. Atmos.* **110** D12110

Badger J, Frank H, Hahmann A N and Giebel G 2014 Wind-climate estimation based on mesoscale and microscale modeling: Statistical-dynamical downscaling for wind energy applications *J. Appl. Meteor. Clim.* **53** 1901–19

Barthelmie R J and Jensen L E 2010 Evaluation of wind farm efficiency and wind turbine wakes at the nysted offshore wind farm *Wind Energy* **13** 573–86

Barthelmie R J, Pryor S C, Frandsen S T, Hansen K S, Schepers J G, Rados K, Schlez W, Neubert A, Jensen L E and Neckelmann S 2010 Quantifying the impact of wind turbine wakes on power output at offshore wind farms *J. Atmos. Ocean. Tech.* **27** 1302–17

Charnock H 1955 Wind stress over a water surface *Q. J. R. Meterol. Soc.* **81** 639–40

EIA 2015 USA energy information administration (https://www.eia.gov/electricity/monthly/epm_table_grapher.cfm?t=epmt_1_01)

EWEA 2016 The european offshore wind industry—key trends and statistics 2015, *Technical report* European Wind Energy Association

Fitch A C, Olson J B, Lundquist J K, Dudhia J, Gupta A K, Michalakes J and Barstad I 2012 Local and mesoscale impacts of wind farms as parameterized in a mesoscale nwp model *Mon. Weather Rev.* **140** 3017–38

GWEC 2016 Global wind statistics 2015, Technical report *Global Wind Energy Council*

Hahmann A N, Vincent C L, Peña A, Lange J and Hasager C B 2015 Wind climate estimation using WRF model output: Method and model sensitivities over the sea *Int. J. Clim.* **35** 3422–39

IEA 2014 International energy agency (http://www.iea.org/statistics/statisticssearch/)

Jacobson M Z and Archer C L 2012 Saturation wind power potential and its implications for wind energy *Proc. Natl Acad. Sci. USA* **109** 15679–84

Jiménez P A, Navarro J, Palomares A M and Dudhia J 2015 Mesoscale modeling of offshore wind turbine wakes at the wind farm resolving scale: a composite-based analysis with the Weather Research and Forecasting model over Horns Rev *Wind Energy* **18** 559–66

LORC 2016 Lorc knowledge (http://www.lorc.dk/offshore-wind-farms-map/horns-rev-1) (Accessed: 10 July 2016)

Lu X, McElroy M B and Kiviluoma J 2009 Global potential for wind-generated electricity *Proc. Natl Acad. Sci. USA* **106** 10933–8

MacKay D J C 2013 Could energy-intensive industries be powered by carbon-free electricity? *Phil. Trans. R. Soc.* A **371** 20110560

Marvel K, Kravitz B and Caldeira K 2013 Geophysical limits to global wind power *Nat. Clim. Change* **3** 118–21

Meyers J and Meneveau C 2012 Optimal turbine spacing in fully developed wind farm boundary layers *Wind Energy* **15** 305–17

Miller L M, Brunsell N A, Mechem D B, Gans F, Monaghan A J, Vautard R, Keith D W and Kleidon A 2015 Two methods for estimating limits to large-scale wind power generation *Proc. Natl Acad. Sci. USA* **112** 11169–74

Mortensen N, Heathfield D, Myllerup L, Landberg L and Rathmann O 2007 Getting Started with WAsP 9, Risø-I *Risø National Laboratory*

Nakanishi M and Niino H 2009 Development of an improved turbulence closure model for the atmospheric boundary layer *J. Meteorol. Soc. Jpn. Ser* **87** 895–912

Petersen E L, Troen I, Jørgensen H E and Mann J 2013 Are local wind power resources well estimated? *Environ. Res. Lett.* **8** 011005

Porté-Agel F, Lu H and Wu Y-T 2014 Interaction between large wind farms and the atmospheric boundary layer *Procedia IUTAM* **10** 307–18

Rados K, Larsen G, Barthelmie R, Schlez W, Lange B, Schepers G, Hegberg T and Magnisson M 2001 Comparison of wake models with data for offshore windfarms *Wind Engineering* **25** 271–80

Rienecker M M and Coauthors 2011 Merra: Nasa's Modern-Era Retrospective Analysis for Research and Applications *J. Climate* **24** 3624–48

Schepers J *et al* 2015 *AVATAR: AdVanced Aerodynamic Tools for lArge Rotors 1 AIAA SciTech* pp 291–310

Skamarock W C, Klemp J B, Dudhia J, Gill D O, Barker M, Duda K G, Huang X Y, Wang W and Powers J G 2008 A description of the advanced research WRF version 3, Technical report *National Center for Atmospheric Research* pp 1–113

van der Laan M P, Sørensen N N, Rthor P-E, Mann J, Kelly M C, Troldborg N, Hansen K S and Murcia J P 2015 The k–fp model applied to wind farms *Wind Energy* **18** 2065–84

Vanderwende B J and Lundquist J K 2012 The modification of wind turbine performance by statistically distinct atmospheric regimes *Environ. Res. Lett.* **7** 034035

Volker P J H, Badger J, Hahmann A N and Ott S 2015 The explicit wake parametrisation v1.0: a wind farm parametrisation in the mesoscale model WRF *Geosci. Model Dev.* **8** 3715–31

Wagner R, Courtney M, Gottschall J and Lindelöw-Marsden P 2011 Accounting for the speed shear in wind turbine power performance measurement *Wind Energy* **14** 993–1004

Wu Y-T and Porté-Agel F 2011 Large-eddy simulation of wind-turbine wakes: evaluation of turbine parametrisations, Bound.-Lay. *Meteorol.* **138** 345–66